The influence of pipe length on turbulence statistics computed from direct numerical simulation data

C. Chin,[1] A. S. H. Ooi,[1] I. Marusic,[1] and H. M. Blackburn[2]
[1]*Department of Mechanical Engineering, University of Melbourne, Victoria 3010, Australia*
[2]*Department of Mechanical and Aerospace Engineering, Monash University, Victoria 3186, Australia*

(Received 25 May 2010; accepted 13 August 2010; published online 9 November 2010)

In this paper, direct numerical simulation of fully developed turbulent pipe flow is carried out at $\mathrm{Re}_\tau \approx 170$ and 500 to investigate the effect of the streamwise periodic length on the convergence of turbulence statistics. Mean flow, turbulence intensities, correlations, and energy spectra were computed. The findings show that in the near-wall region (below the buffer region, $r^+ \leq 30$), the required pipe length for all turbulence statistics to converge needs to be at least a viscous length of $O(6300)$ wall units and should not be scaled with the pipe radius (δ). It was also found for convergence of turbulence statistics at the outer region that the pipe length has to be scaled with pipe radius and a proposed pipe length of $8\pi\delta$ seems sufficient for the Reynolds numbers considered in this study. © *2010 American Institute of Physics*. [doi:10.1063/1.3489528]

I. INTRODUCTION

With the advancement in computer technology, data obtained from direct numerical simulation (DNS) of turbulent flows are fast becoming an indispensable tool for turbulence research.[1] The use of DNS provides a vast amount of information for scientists to better understand the physics of turbulent flows. The earliest reported study of DNS is of three-dimensional isotropic turbulence by Orszag and Patterson[2] more than three decades ago. Since then, low Reynolds number DNS of turbulent boundary layer, channel, and pipe flows has been performed by various workers. As the Reynolds number of DNS is now approaching and overlapping the lower end portion of experimental Reynolds number range, it is possible to compare statistics between them. However, statistics are influenced by how the boundary conditions interact with the largest scale motion in DNS. Since the early hot-wire experiments of Favre *et al.*[3] and Townsend[4] it has been well known that long streamwise correlations exist in wall-bounded turbulent flows. A renewed interest in this topic came with the experiments by Kim and Adrian[5] who highlighted that the inferred length of these motions in turbulent pipe flows from premultiplied spectra were considerably longer than previously appreciated. (Marusic *et al.*[6] provides a review of these studies). Balakumar and Adrian[7] also reviewed the available data and designated "large-scale motions" (LSMs) as motions with wavelength of up to $2-3\delta$, where δ is the half channel height, pipe radius or boundary later thickness, and very-large-scale motions (termed VLSMs with wavelength of more than 3δ) to be present within the outer flow. Another study by Hutchins and Marusic[8] reported long meandering features in the logarithmic region of turbulent boundary layers to exceed 20δ. It was later reported by Monty *et al.*[9,10] that these long meandering features in pipe and channel are up to 25δ in length. They also reported that coherent structures in turbulent boundary layers are smaller in maximum streamwise and spanwise extents than turbulent pipe and channel flows. Hence internal flow simulations are liable to require more extended domains than comparable flat wall boundary layer flows. In this paper, we will investigate the length of domain required in order to obtain converged statistics.

One of the earliest DNS of internal flow was that of a turbulent channel flow, carried out by Kim *et al.*[11] at $\mathrm{Re}_\tau = u_\tau \delta/\nu \approx 180$ (where u_τ is the friction velocity, ν is the kinematic viscosity). They compared DNS results with experimental data and found that general characteristics of turbulence statistics are in agreement except at the near-wall region. It was suspected that the disagreement might be due to the inaccurate measurement of the experimental u_τ. The computational domain size was chosen to be $4\pi\delta \times 2\pi\delta \times 2\delta$ (streamwise, spanwise, and wall normal). Like most DNS studies of fully developed turbulent channel and pipe flows, streamwise periodicity was employed in their simulation. This is justifiable if the computational domain is sufficiently long that the largest eddies are fully represented and the velocity fluctuations are uncorrelated at the half domain period.[11] Kim *et al.*[11] showed that the velocity correlations were uncorrelated (Fig. 2 of their paper) to justify their choice of domain streamwise extend. Eggels *et al.*[12] performed DNS of turbulent pipe flow at Re_τ of 180 to investigate the differences between channel and pipe flows and to compare with experimental results. They also utilized streamwise periodicity with a computational pipe length of 10δ. This length was chosen on the same basis as used by Kim *et al.*[11] However, Eggels *et al.*[12] reported correlations being nonzero at streamwise separation of half the pipe length, which suggests that their pipe length may have been insufficient. They did not investigate how other statistics were affected by domain length, which is what our present study will address. Though correlation statistics serve as a guideline when choosing a suitable length for DNS, there is no benchmark regarding the computational size requirement to fully isolate the effects of streamwise periodicity.

Following these pioneering DNS studies of channel and pipe flows, many further investigations have been carried

out, with Reynolds numbers generally rising with time as a result of increased computational power. Low Reynolds numbers tend to decrease near-wall values of rms values of turbulent fluctuations. This has been documented by Antonia and Kim[13] using DNS channel flow at $\mathrm{Re}_\tau \approx 180$ and 400 at domain length of $4\pi\delta$. Other DNS of turbulent channel flow studies include those of Moser *et al.*[14] at $\mathrm{Re}_\tau \approx 180$, 395, and 590 with corresponding computational domain sizes of $4\pi\delta \times 4/3\pi\delta \times 2\delta$, $2\pi\delta \times \pi\delta \times 2\delta$, and $2\pi\delta \times \pi\delta \times 2\delta$. Iwamoto *et al.*[15] computed DNS channel flow at $\mathrm{Re}_\tau \approx 110$ at $5\pi\delta \times 2\pi\delta \times 2\delta$ and at $\mathrm{Re}_\tau \approx 150$, 300, 400, and 650 with constant domain size $2.5\pi\delta \times 2\pi\delta \times 2\delta$. Abe *et al.*[16] also used DNS channel flow at $\mathrm{Re}_\tau \approx 180$, 395, and 640 at different box sizes of $12.8\delta \times 6.4\delta \times 2\delta$, $6.4\delta \times 3.2\delta \times 2\delta$, and $6.4\delta \times 2\delta \times 2\delta$, respectively. Later, Abe *et al.*[17] recognized that the effects of large-scale structures in the outer region require a larger domain size to capture large-scale features. They carried out a study at the same Reynolds numbers and kept the box sizes constant at $12.8\delta \times 6.4\delta \times 2\delta$ to investigate large-scale features. Hoyas and Jiménez[18] carried out DNS of channel flow at $\mathrm{Re}_\tau \approx 2003$. In that paper, they compared DNS results with previous published channel flow of $\mathrm{Re}_\tau \approx 547$ and 934,[19] all with a domain length of $8\pi\delta$. Hoyas and Jiménez[18] showed that the streamwise turbulence intensities, normalized with inner variable, increase with Reynolds number across the entire boundary layer.

For pipe flow simulations, unlike those for channel and boundary layer flows, a natural periodicity exists and only the streamwise domain size needs consideration. Reynolds number effect in turbulent pipe flow is of particular interest to many due to the natural periodicity in the azimuthal direction. Wanger *et al.*[20] performed a DNS of turbulent pipe flow with Reynolds number from $\mathrm{Re}_\tau \approx 180$, 250 and 320 with fixed pipe length of 10δ, however no details on why they chose this pipe length was given. The reported results were in agreement with the reports[14,16] for channel flow where rms of velocity fluctuations increases with Reynolds number. More recently, DNS of higher Reynolds number turbulent pipe flows have been made available by Wu and Moin[21] where the simulation is based on a pipe length of 15δ at $\mathrm{Re}_\tau \approx 1142$. They chose this pipe length based on previous findings in the literature that reported LSMs to range between 8δ and 16δ.[22,23]

As evidenced from the discussion above, computational domain sizes in pipe and channel flows vary considerably. There has been an inclination towards running simulations at higher Reynolds numbers at the expense of shortening the domain length. This is no coincidence because the computational cost of a wall-bounded numerical simulation as estimated by Jiménez[24] scale with $\sim L_x^2 L_y \mathrm{Re}_\tau^4$. For example, if we could afford a n-fold increase in computational time, there is a strong temptation to increase Re_τ by factors of $\sqrt{n}$ rather than increasing the domain length L_x by factors of n. Most early simulations were for domains restricted to $2\pi\delta$ and more recently del Álamo *et al.*[19] and Hoyas and Jiménez[18] have advocated the need for longer channels, up to $8\pi\delta$. Figure 1 summarizes the streamwise domain extents for selected DNS studies of channel and pipe flows. Figure 1(a) shows the computational lengths of the simulations scaled with δ. The upper bound on the streamwise extent (l) for these previous works, all with $\mathrm{Re}_\tau < 1000$, is 40δ. When the computational lengths are plotted in terms of wall units ($l^+ = l u_\tau/\nu$) as shown in Fig. 1(b), we see an increase in computational length over two orders of magnitude. It is well known that the most energetic small-scale structures have a streamwise wavelength of $\lambda_x^+ \approx 1000$ (Ref. 6) and if the computational domain is less than $l^+ = 1000$, the influences of streamwise periodicity are substantial as will be shown later in this study.

Up to now, there are very limited studies that have looked at the effects of the computational domain length, with the exception of the study of del Álamo *et al.*[19] where the effects of reduced computational box size were briefly discussed. As will be shown later in this article, effects of computational length can cause a variation of turbulence statistics for pipe flow and would render comparison of different DNS data sets inaccurate. Thus, the objective of this study is to investigate the effects of computational domain length on turbulence statistics and determine the minimum lengths required for various statistics to converge. Low-order turbulence statistics such as mean flow and turbulence intensities are dealt with first, followed by higher order turbulence statistics such as two-point correlations, cross correlations, and one-dimensional energy spectra. The Reynolds numbers chosen for the study are $\mathrm{Re}_\tau \approx 170$ and 500.

II. METHODOLOGY

The governing equations considered in the simulations are the incompressible Navier–Stokes equations coupled with the continuity equation

$$\frac{\partial \boldsymbol{u}}{\partial t} + \mathbf{N}(\boldsymbol{u}) = -\rho^{-1}\nabla p + \nu\nabla^2 \boldsymbol{u}, \tag{1}$$

$$\nabla \cdot \boldsymbol{u} = 0. \tag{2}$$

The equations are written in the cylindrical coordinate system and we will use x, r, and θ to denote the axial, radial, and azimuthal directions, respectively. The velocity components $\boldsymbol{u}$ (u, u_r, and u_θ) and pressure (p) are functions of (x, r, θ, t). The nonlinear terms are denoted by $\mathbf{N}(\boldsymbol{u})$ which is computed in skew-symmetric form $(\boldsymbol{u}\cdot\nabla\boldsymbol{u} + \nabla\cdot\boldsymbol{u}\boldsymbol{u})/2$ for robustness. The numerical scheme employed is detailed in Blackburn and Sherwin[25] and is based on a cylindrical-coordinate spectral element/Fourier spatial discretization. The velocity $\boldsymbol{u}$ can be directly projected onto a set of two-dimensional complex azimuthal Fourier modes

$$\widehat{\boldsymbol{u}}_k(x,r,t) = \frac{1}{2\pi}\int_0^{2\pi} \boldsymbol{u}_k(x,r,\theta,t) e^{-ik\theta} d\theta, \tag{3}$$

where k is the azimuthal wavenumber. The time integration scheme is based on a second-order velocity-correction projection scheme described by Guermond and Shen[26] and Karniadakis *et al.*[27] Details of the computational domains are presented in Table I. The number of turnovers for each test case is given as TU_b/L_x, where T is the time duration where the statistics were collected and computed, and U_b is the bulk velocity. The grid spacing in the axial and azimuthal direc-

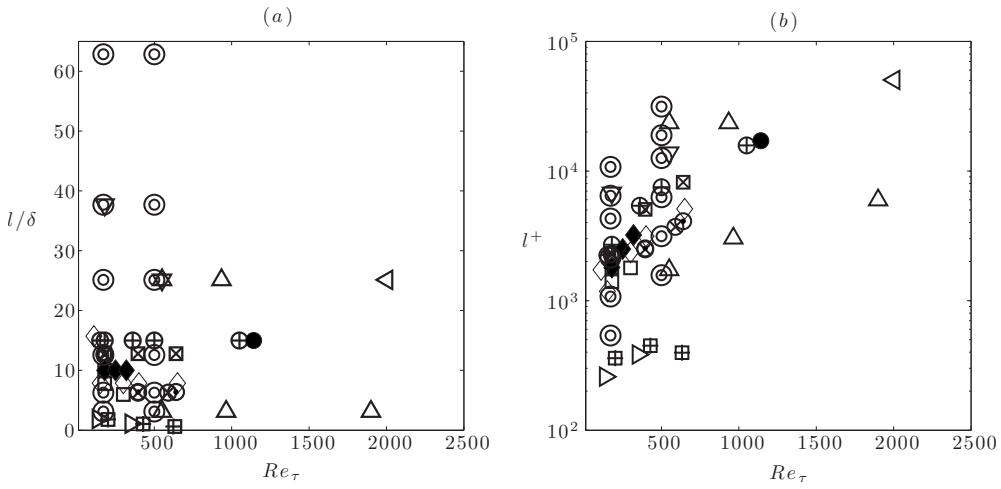

FIG. 1. Previous wall-bounded DNS studies; (a) scaled with δ (half channel height or pipe radius) and (b) scaled in wall units (ν/u_τ).

tions for each Reynolds number are kept constant to ensure that any variation in the data is due to variation in the pipe length (Table I). We have also performed separate calculations to ensure that the grid spacing in all directions are sufficient to resolve all length scales for the Reynolds numbers considered in this study. For both Reynolds numbers of $\mathrm{Re}_\tau \approx 170$ and 500, the pipe lengths range from $\pi\delta$ (shortest) to $20\pi\delta$ (longest). The motivation for choosing these pipe length limits is to enable our study of pipe length effects to encompass the majority of computational domain lengths of previous DNS studies at comparable Reynolds number and to capture the LSMs and VLSMs as discussed earlier. Figure 1 clearly shows the different pipe lengths used (denoted as "◎" symbols) in this study relative to other DNS studies. The spatial resolution in the streamwise direction is kept constant meaning that as the pipe length increases, more elements are added to extend the pipe rather than increasing the grid points and changing the spatial resolution. The spacing (Δr^+) in the radial direction for $\mathrm{Re}_\tau \approx 170$ is 0.5 for the near wall and 3.6 near the pipe center. The radial spacing for

TABLE I. Summary of computational domain and grid information.

Re_τ	170	500
Pipe length (L_x)	$(\pi\delta, 2\pi\delta, 4\pi\delta, 8\pi\delta, 12\pi\delta, 20\pi\delta)$	$(\pi\delta, 2\pi\delta, 4\pi\delta, 8\pi\delta, 12\pi\delta, 20\pi\delta)$
N_x	[8, 16, 32, 64, 96, 160]	[23, 46, 92, 194, 276, 460]
N_r	8	16
N_θ	128	384
Δx^+	6.7	6.8
Δr^+	[0.5, 3.6]	[0.07, 5.5]
$\Delta r\theta^+$ (at wall)	8.4	8.2
TU_b/L_x	[500, 150, 71, 30, 37, 35]	[108, 41, 22, 11, 8, 8]

TABLE II. Summary of computational methods and spatial information for DNS studies listed in Fig. 1.

	Discretization		Spatial resolution			
Previous DNS	Streamwise and spanwise	Wall-normal or radial	Δx^+	$\Delta z^+/\Delta r^+$	$\Delta y^+/\Delta(r\theta)^+$	Re_τ
Channel flows						
Kim *et al.*[a]	Spectral	Spectral	12	[0.05,4.4]	7	180
Antonia *et al.*[b]	Spectral	Spectral	[7,11]	[0.05,5.5]	4	[180,300]
Jiménez and Pinelli[c]	Spectral	Spectral	[9.3,14]	[0.05,7.7]	[3.5,8]	[201,633]
Moser *et al.*[d]	Spectral	Spectral	[9.7,17.7]	[0.04,7.2]	[4.8,6.5]	[180,590]
Abe *et al.*[e]	Second order	Second order	[8,9.88]	[0.15,9.64]	[4.5,5]	[180,640]
del Álamo and Jiménez[f]	Spectral	Spectral	8.9	[0.04,6.7]	4.5	[180,550]
Abe *et al.*[g]	Fourth order	Second order	[8,9.88]	[0.15,8.02]	[4,4.94]	[180,640]
Iwamoto *et al.*[h]	Spectral	Spectral	[16.4,36]	[0.03,7.98]	[5.3,14.4]	[110,600]
Toh and Itano[i]	Spectral	Spectral	13.5		5.4	[137,349]
del Álamo *et al.*[j]	Spectral	Spectral	[7.8,8.9]	[0.02,7.8]	[3.9,4.5]	[550,1900]
Hoyas and Jiménez[k]	Spectral	Fourth order	8.2	[0.02,8.9]	4.1	2003
Pipe flows						
Eggels *et al.*[l]	Second order	Second order	7.03	1.88	8.84	180
Satake *et al.*[m]	Second order	Second order	[8.78,15.4]	[0.1,4.16]	[7.4,8.8]	[150,1050]
Wagner *et al.*[n]	Second order	Second order	[3.7,6.58]	[0.36,7.68]	[4.7,8.4]	[180,320]
Wu and Moin[o]	Second order	Second order	[5.31,8.37]	[0.17,11.3]	[2.2,7.0]	[180,1142]
Current Study	Spectral	Spectral	[6.7,6.8]	[0.07,5.5]	[8.2,8.4]	[170,500]

[a]Reference 11.
[b]Reference 28.
[c]Reference 29.
[d]Reference 14.
[e]Reference 16.
[f]Reference 30.
[g]Reference 17.
[h]Reference 15.
[i]Reference 31.
[j]Reference 19.
[k]Reference 18.
[l]Reference 12.
[m]Reference 32.
[n]Reference 20.
[o]Reference 21.

$\mathrm{Re}_\tau \approx 500$ is 0.07 at the near wall but near the center, the grid spacing is 5.5. The radial grid spacing close to the center of the pipe is comparable to Wu and Moin[21] with $\Delta r^+ \approx 11.3$ at $\mathrm{Re}_\tau \approx 1142$ and Wanger *et al.*[20] with $\Delta r^+ \approx 7.68$ at $\mathrm{Re}_\tau \approx 320$. Table II shows a comparison of computational methods and spatial information for all DNS studies shown in Fig. 1.

III. RESULTS AND DISCUSSIONS

A. Mean velocity profiles

In Fig. 2 the mean velocity profiles are shown for all pipe lengths investigated for both Reynolds numbers. Figures 2(a) and 2(c) show the mean velocity profiles normalized by the center velocity U_c from the pipe center $(r/\delta = 0)$ to the wall $(r/\delta = 1.0)$. Figures 2(b) and 2(d) show the mean velocity profiles normalized by the friction velocity as a function of wall-normal locations (where $r^+ = 0$ is at the wall). The results from $\mathrm{Re}_\tau \approx 170$ show the lack of convergence for the mean velocity profile at pipe length of $\pi\delta$ whereas the results for $\mathrm{Re}_\tau \approx 500$ show no discrepancy for all pipe lengths considered. The pipe lengths required for convergence seem to differ when scaled with δ, but when the pipe length is measured in wall units, for $\mathrm{Re}_\tau \approx 170$, convergence of the data starts when the pipe length is $2\pi\delta$, which is approximately 1000 wall units, and for $\mathrm{Re}_\tau \approx 500$, $\pi\delta$ is approximately 1500 wall units. This suggests that mean velocity profiles seem to collapse when the pipe length $l^+ > O(1000)$. The effect of domain length on the Reynolds shear stress $(-\overline{u'u_r'^+})$ profiles has also been investigated and the convergence of this statistic was found to be very similar to the convergence of the mean velocity profiles.

B. Turbulence intensity profiles

The rms statistics for the streamwise fluctuating velocity, here defined by u', for different pipe lengths are shown in Figs. 3(a) and 3(b) for $\mathrm{Re}_\tau \approx 170$ and 500, respectively. Here the rms is normalized by the friction velocity $(u'^+ = u'/u_\tau)$. It is clearly shown that the u'^+ profile for $\pi\delta$ for both Reynolds numbers differs from the other pipe lengths. At $\mathrm{Re}_\tau \approx 170$, the statistics for pipe length of $2\pi\delta$ also seem to differ slightly. Figures 3(c) and 3(d) show the turbulence intensity at a chosen wall-normal location of $r^+ \approx 15$. This height is chosen due to the well known fact that the peak turbulence intensity occurs at this wall-normal height. The converged peak turbulence intensities for $\mathrm{Re}_\tau \approx 170$ and 500 are $u'^+ \approx 2.6$ and 2.7, respectively. This increase in turbulence intensity as the Reynolds number increases is widely accepted as a Reynolds number effect.[19,33–35] Here it is highlighted that the minimum length required for u'^+ to converge within 1% variation (shown as dashed lines) of the value of u'^+ calculated for the longest four pipe lengths for each Reynolds number. For $\mathrm{Re}_\tau \approx 170$, the minimum length is $4\pi\delta$ corre-

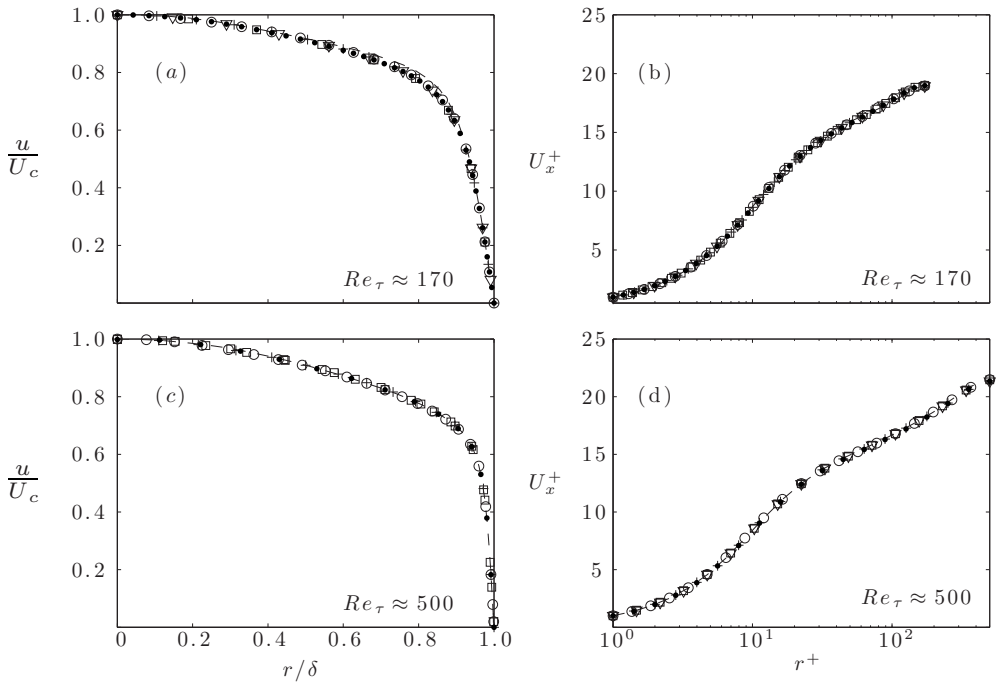

FIG. 2. Streamwise mean velocity profile (u); (a) and (c) normalized by center-line velocity U_c and (b) and (d) normalized by the friction velocity u_τ. The symbols used are the same for both Re_τ to represent different pipe lengths; $\pi\delta$ (– –), $2\pi\delta$ (○), $4\pi\delta$ (+), $8\pi\delta$ (□), $12\pi\delta$ (▽), $20\pi\delta$ (●).

sponding to $l^+ \approx O(2100)$ and for $\mathrm{Re}_\tau \approx 500$, the length required is $2\pi\delta$ corresponding to $l^+ \approx O(3100)$. It is apparent from Figs. 3(a) and 3(b) that an artifact of insufficient pipe length is a higher value in the peak turbulence intensity (at $r^+ = 15$). This finding is consistent with Toh and Itano[31] who reported a higher than expected peak turbulence intensity for DNS of short channel flow. In their paper, the peak intensity is $u'^+ \approx 3$ for $\mathrm{Re}_\tau \approx 137$ and channel length of $l^+ \approx 259$, which is relatively close to our result of $u'^+ \approx 2.9$ with Reynolds number of $\mathrm{Re}_\tau \approx 170$ and pipe length of $l^+ \approx 534$. We

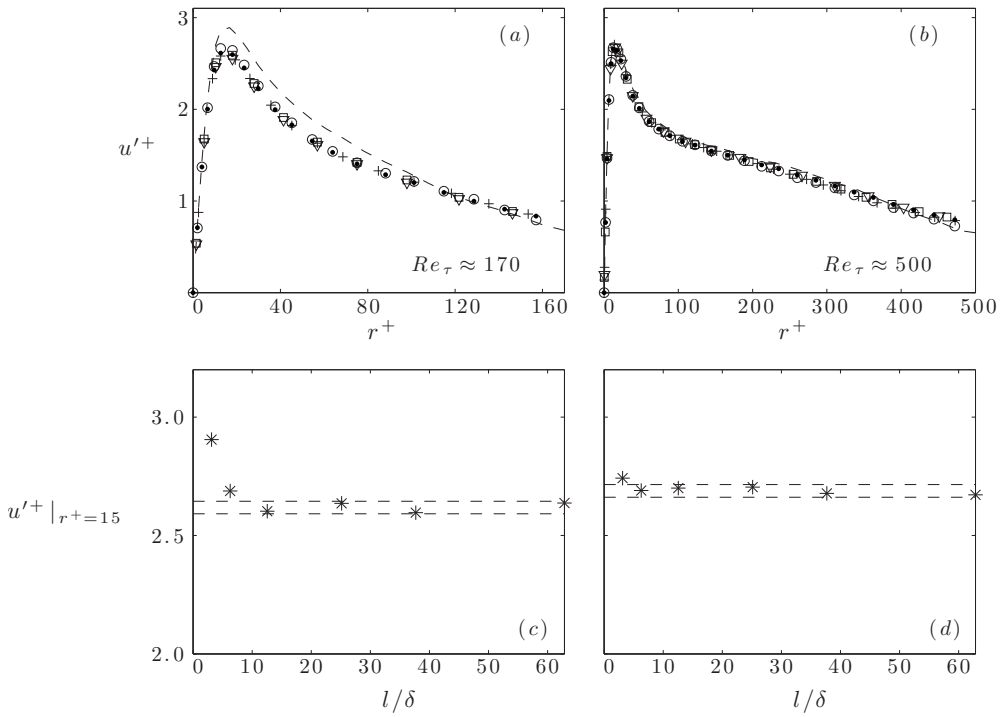

FIG. 3. Streamwise velocity turbulence intensity profile u'^+ for different pipe lengths, (a) for $\mathrm{Re}_\tau \approx 170$ and (b) for $\mathrm{Re}_\tau \approx 500$. Symbols used in (a) and (b) are as in Fig. 2. (c) and (d) shows the turbulence intensity at wall-normal location $r^+ \approx 15$ for different pipe lengths. The two dashed lines in (c) and (d) represent 1% variation from the mean of u'^+ based on the four longest pipe lengths.

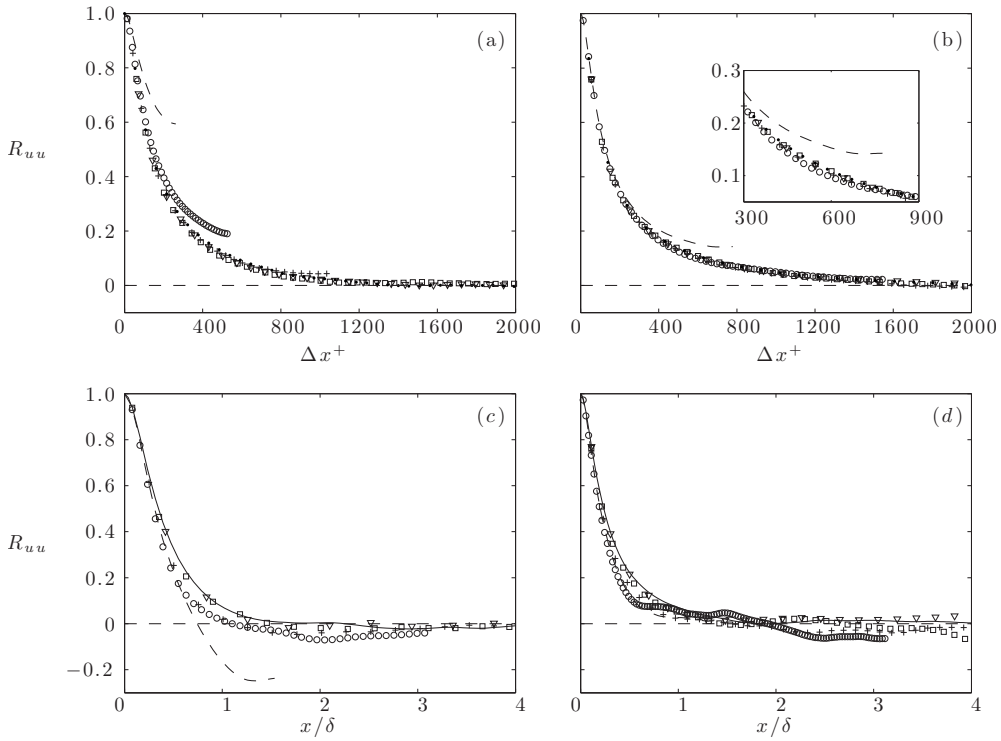

FIG. 4. Streamwise two-point correlation for velocity (u) at wall-normal location $r^+ \approx 15$ for different pipe lengths, (a) for $\mathrm{Re}_\tau \approx 170$ and (b) for $\mathrm{Re}_\tau \approx 500$. (c) and (d) show the two-point correlation at $r/\delta \approx 0.9$ for $\mathrm{Re}_\tau \approx 170$ and 500, respectively. The x-axes for (a) and (b) are in viscous length scale and for (c) and (d) are normalized by δ. Symbols used are as in Fig. 2.

will try to quantify why a greater peak turbulence intensity occurs for shorter pipes using correlation functions which we will discuss in the next section.

C. Streamwise two-point correlations

In addition to the use of two-point correlations as an aid in choosing a suitable computational length, they have also been used to understand average structure characteristics and help identify coherent structures. The correlation between any two fluctuating components I and J is defined as

$$R_{IJ} = \frac{\overline{I(x,r\theta,r)J(x+\Delta x, r\theta+\Delta r\theta, r)}}{\sigma_I \sigma_J}, \tag{4}$$

where σ refers to the standard deviation, and Δx and $\Delta r\theta$ are the spatial distances in the streamwise and azimuthal directions, respectively; r is the desired wall-normal location. The overbar denotes the spatial average. Correlation functions have successfully been employed by Ganapathisubramani *et al.*[36] to identify and study vortical structures and also by Hutchins and Marusic[8] to study large-scale features of atmospheric surface layer structures, which they termed "superstructures."

Two-point correlation results for different pipe lengths are shown in Fig. 4. Figure 4(a) shows the results at wall-normal location $r^+ \approx 15$ for $\mathrm{Re}_\tau \approx 170$. As the pipe length increases, the correlation curves start to extend axially and fall off towards zero. When the pipe length is $8\pi\delta$, the correlation falls completely to zero and similar results are obtained for pipe lengths of 12 and $20\pi\delta$. This shows that convergence is achieved at a pipe length of $8\pi\delta$. Results for the same Reynolds number at another wall-normal location nearer to the pipe center $r/\delta \approx 0.9$ are shown in Fig. 4(c). Here the correlation curves fall sharply and cross $R_{uu}=0$ at a smaller Δx^+ (all curves cross before $\Delta x^+ < 500$ which is $x/\delta < 3$) as compared to the correlation curves in Fig. 4(a). The correlation curve for $\pi\delta$ crosses zero at $x/\delta \approx 0.8$, for 2 and $4\pi\delta$, and correlation curves cross zero at $x/\delta \approx 1$. Results start to converge and cross zero at $x/\delta \approx 1.5$ when the pipe length is $8\pi\delta$ and greater. Correlation curves that do not cross the $R_{uu}=0$ suggest that there is a periodicity effect, which will be discussed in the next section. Results for $\mathrm{Re}_\tau \approx 500$ at $r^+ \approx 15$ is shown in Fig. 4(b). The results seem to suggest that convergence is achieved at a pipe length of $2\pi\delta$. However, the inserted diagram in Fig. 4(b) clearly shows that the statistics are not yet converged at $2\pi\delta$ and that convergence is only achieved at $4\pi\delta$. The results at wall-normal location $r/\delta \approx 0.9$ are shown in Fig. 4(d) and the pipe length required for convergence of statistics is $8\pi\delta$. It is interesting to note the result for $\mathrm{Re}_\tau \approx 170$ for $2\pi\delta$ is similar to that for $\mathrm{Re}_\tau \approx 500$ at $\pi\delta$. In viscous length scale, this is $l^+ \approx O(1100)$ and $O(1600)$ for corresponding $\mathrm{Re}_\tau \approx 170$ and 500. In terms of viscous units, both Reynolds numbers in the near-wall region require $l^+ \approx O(4300)$ and $O(6300)$ for $\mathrm{Re}_\tau \approx 170$ and 500, respectively. This illustrates that if a similar pipe length (in viscous units) is used, even at different Reynolds numbers, the pipe length required to achieve convergence of the statistics would not vary significantly. In the outer-region near the pipe center, the pipe length required for convergence is $8\pi\delta$ for both Reynolds numbers. This sug-

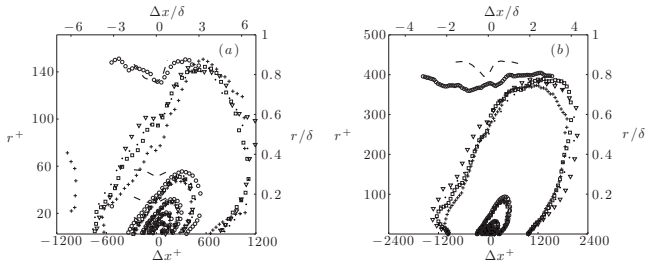

FIG. 5. Streamwise cross correlation between streamwise velocity (u) and streamwise wall shear stress (τ) for wall-normal locations from wall to pipe center, (a) for $\mathrm{Re}_\tau \approx 170$ and (b) for $\mathrm{Re}_\tau \approx 500$. Contour lines are from 0.03 (outermost) with increment of 0.2. Symbols used for (a) and (b) are the same and as in Fig. 2.

gests that pipe length requirement in near-wall statistics should be in viscous units while the outer region has to be scaled with δ.

D. Cross correlations for streamwise velocity

Cross correlation functions support the hypothesis of the existence of coherent and organized structures in wall-bounded turbulent flows as reported in the literature.[17,37–39] The cross correlations between streamwise velocity u and streamwise wall shear stress τ for wall-normal location up to the pipe center are shown in Fig. 5. Here we have plotted the contours of the correlation coefficient, $R_{u\tau}$, as a function of wall-normal location (r^+) and streamwise separation distance (Δx^+). The normalized wall-normal distance (r/δ) and streamwise separation distance ($\Delta x/\delta$) are included for comparison between both Reynolds numbers. Here the correlation contour lines begin at a value of 0.03 at the outermost contour and increase at intervals of 0.2. The results for $\mathrm{Re}_\tau \approx 170$ are shown in Fig. 5(a) and for $\mathrm{Re}_\tau \approx 500$ in Fig. 5(b). One should note that the cross correlation contours for the different pipe lengths are plotted in the same figure and the abrupt end of contour lines for pipe lengths $\pi\delta$, $2\pi\delta$, and $4\pi\delta$ in Fig. 5(a) signify the axial limits of the computational domain. The contour lines (for $\pi\delta$ and $2\pi\delta$) that do not close strongly suggest "contamination" of structures in the flow (in an average sense) owing to the periodicity in the streamwise direction. This is due to a pipe length that is too short to accommodate the longest structures in the flow field. This translates to the structures being infinitely long and having a constant influence on the streamwise wall shear stress. Looking at the contours for $l/\delta = 4\pi\delta$, the outermost contour line ($R_{u\tau}=0.03$) fails to form a complete curve at $\Delta x^+ \approx 1100$ and the missing bit of the contour line is seen at $\Delta x^+ \approx -1100$. As mentioned, this is due to periodicity of the structures and it can be interpreted as the leading tip of the structures leaving one end of the pipe and coming back at the other end. This periodic cycle of structures is the reason the correlation curves in Fig. 4 do not cross $R_{uu}=0$ for pipe lengths less than $4\pi\delta$. The cross correlation statistics start to converge as the pipe length exceeds $8\pi\delta$. In Fig. 5(b), the moderate Reynolds number case exhibits similar effects of insufficient pipe length as for $\mathrm{Re}_\tau \approx 170$ [Fig. 5(a)]. However, in this case, the cross correlation statistics start to converge at $4\pi\delta$. Once again if we relate the minimum pipe length required for convergence for both Reynolds numbers in viscous length scale, for $\mathrm{Re}_\tau \approx 170$ we would need $l^+ \approx O(4300)$ and for $\mathrm{Re}_\tau \approx 500$, $l^+ \approx O(6300)$ is required. The correlation contours show that there is correlation even at distances far from the wall for pipe lengths of $\pi\delta$ and $2\pi\delta$ for both Reynolds number discussed. Results from the turbulence intensity and correlation profiles suggest that statistics near the wall should be scaled in terms of viscous wall units rather than the outer scaling δ. This gives a better benchmark for the pipe length requirement for convergence of statistics.

Contours of streamwisely averaged azimuthal cross correlation between streamwise velocity u and streamwise wall shear stress τ are shown in Fig. 6. Figure 6(a) shows the results for $\mathrm{Re}_\tau \approx 170$ and Fig. 6(b) for $\mathrm{Re}_\tau \approx 500$. The left hand side of the figure displays the result for $\pi\delta$ and the right hand side the result for $20\pi\delta$. The correlation coefficient is shown as gray contour lines and shaded contours. The contour lines vary from 0.1 from the outermost contour with an increment of 0.2. The contour shading has been adjusted to provide a clearer picture of pipe length effects on the correlation statistics, red denotes positive correlation, and blue

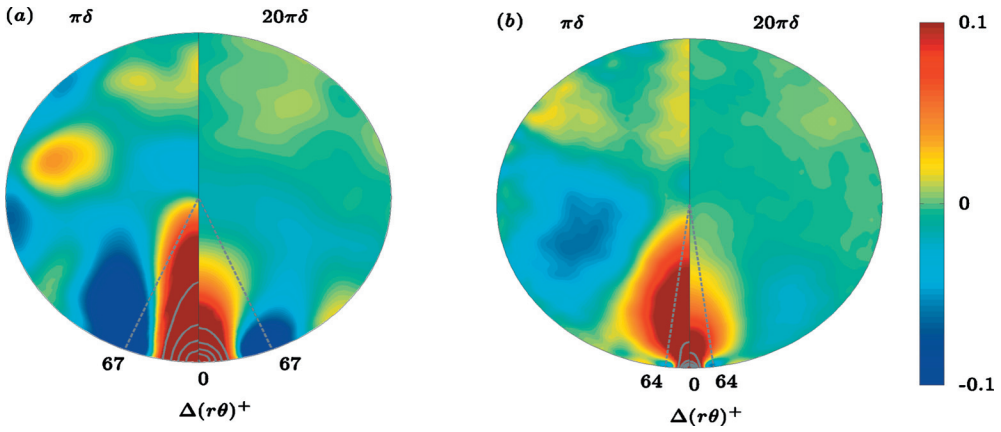

FIG. 6. (Color) Contours of streamwisely averaged azimuthal cross correlation between streamwise velocity (u) and streamwise wall shear stress (τ) for wall-normal locations from wall to pipe center, (a) for $\mathrm{Re}_\tau \approx 170$ and (b) for $\mathrm{Re}_\tau \approx 500$. Contour shadings vary from negative correlation −0.1 (blue) to positive correlation 0.1 (red). Contour lines (gray) are from 0.1 (outermost) with increment of 0.2. The dashed lines show the approximate azimuthal distances ($\Delta(r\theta)^+$) of the peak negative correlation.

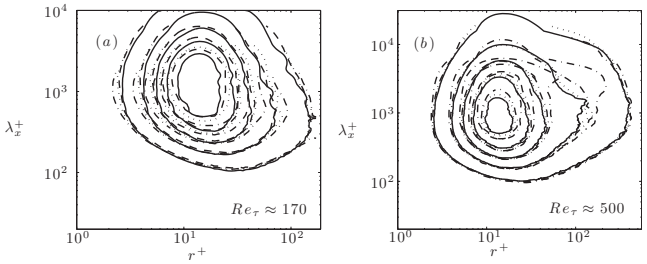

FIG. 7. One-dimensional normalized streamwise premultiplied energy spectra for streamwise velocity u for all wall-normal locations r^+ for (a) $\mathrm{Re}_\tau \approx 170$ and (b) $\mathrm{Re}_\tau \approx 500$. The y-axis is the normalized streamwise wavelength $\lambda_x^+ = \lambda_x u_\tau / \nu$. Contour lines are from 0.3 (outermost) with increment of 0.4. The symbols used are $4\pi\delta$ (dot-dashed line – — –), $8\pi\delta$ (dotted line ·····), $12\pi\delta$ (dashed-line – –), and $20\pi\delta$ (solid line ——).

denotes negative correlation. The results clearly illustrate the averaged structure size (radially) is bigger for a short pipe length (due to the periodicity in the streamwise direction) as compared to a pipe length that is sufficiently long. This agrees with the streamwise cross correlation results previously discussed. The distinctive positive-negative-positive correlation indicates existence of counter rotating vortex pairs (in an averaged sense). Interestingly the peak negative correlation at the near wall is at an azimuthal separation distance of $\Delta(r\theta)^+ \approx O(60)$ and the azimuthal extent of positive correlation is about $(r\theta)^+ \approx O(100)$, for both Reynolds numbers at pipe lengths of $\pi\delta$ and $10\pi\delta$. This positive correlation extent can be taken as representative of eddies with azimuthal wavelength of $\lambda^+ \approx 100$. This wavelength of $\lambda^+ \approx 100$ corresponds to the average spanwise wavelength of near-wall dominant structures[40] and can also be seen in the two-dimensional energy spectra map of Hoyas and Jiménez.[18]

From both the streamwise and azimuthal cross correlations, we can infer that turbulent structures in an average sense span up to the center of the pipe for short computational pipe lengths and these massive periodic structures are most likely the contributing factor to the greater peak turbulence intensity seen in Figs. 3(a) and 3(b).

E. One-dimensional premultiplied streamwise energy spectra

Energy spectra are often used to express the energy contribution of structures for wavelengths λ_x at a given wall-normal distance. Premultiplied energy spectra are calculated using

$$\Psi_{uu}(k_x, r) = k_x \langle \hat{u}(k_x, r) \hat{u}^*(k_x, r) \rangle, \tag{5}$$

where k_x is the streamwise wavenumber, $\langle\ \rangle$ denotes spatial and temporal averaging, $\hat{u}$ denotes Fourier transform of u, and * denotes complex conjugate. Figure 7 presents contours of the normalized one-dimensional, premultiplied streamwise energy spectra ($\Psi^+ = \Psi / u_\tau^2$) of the streamwise velocity component u. In Fig. 7, we emphasize only the energy spectra for pipe lengths of 4, 8, 12, and $20\pi\delta$ for both $\mathrm{Re}_\tau \approx 170$ and 500. These pipe lengths are chosen because the turbulence statistics computed in the previous sections indicated lack of convergence for pipe lengths up to $2\pi\delta$. The energy spectra are plotted as a function of streamwise wavelength λ_x, where $\lambda_x = 2\pi / k_x$. The results for $\mathrm{Re}_\tau \approx 170$ show convergence for the pipe lengths exceeding $8\pi\delta$ or a viscous length of $O(4300)$. In Fig. 7(b), the energy spectra for $4\pi\delta$ converges in the near-wall region ($r^+ < 20$) and fails to converge at distances further away from the wall. The reason for the lack of convergence away from the wall is due to the insufficient pipe length. This causes the energy which is supposed to be contained within the large-scale structures to be redistributed to the small scales as seen in Fig. 7(b) in the region of r^+ of 20–200. The energy spectra for $8\pi\delta$–$20\pi\delta$ seem to converge nicely, suggesting a pipe length of $8\pi\delta$ or a viscous length of $O(12\,000)$ is sufficient for the analysis of energy spectra statistics.

Figure 7 clearly shows a distinctive peak in the energy spectra at location $r^+ \approx 15$, $\lambda_x^+ \approx 1000$ as has been well noted in the literature.[6] Hutchins and Marusic[8,41] and Monty *et al.*[10] have also noted an outer peak in such premultiplied spectral plots occurring in the logarithmic region at wavelengths of $6\pi\delta$ (corresponding to the VLSM or superstructures), but no such peak is discernible here. However, it is noted that the Reynolds numbers are very low, and effectively there is a very small separation of length scales. Correspondingly, there is a lack or nonexistence of the logarithm region at the Reynolds numbers considered in this study. Evidence from the energy spectra statistics seems to indicate that in the near-wall region, a pipe length of $l^+ \approx O(6300)$ is sufficient for convergence for both Reynolds numbers. Results also show that a pipe length of $8\pi\delta$ is sufficient for the energy spectra statistics to be independent of Reynolds number and wall-normal distance.

IV. CONCLUSIONS

In this study, the effects of periodic domain length on turbulence statistics were investigated for various computational pipe lengths. The influence of insufficient pipe length on the convergence of lower order statistics (such as the mean velocity profile) is less significant as compared to higher order statistics (such as correlations and energy spectra). Our results show that an artifact of a short pipe length [$l^+ < O(3100)$] is the periodicity of structures in the flow, resulting in artificial domain-filling structures contributing to greater turbulence intensities.

The minimum computational pipe lengths required for convergence for various turbulence statistics for both Reynolds numbers are summarized in Table III. The table displays the different turbulence statistics calculated and highlights the required minimum lengths in terms of pipe radius (δ) and viscous length scale ($^+$). For the one-dimensional energy spectra statistics, the minimum length to obtain converged results for $r^+ < 20$ is stated in the brackets "( )." The conclusion that can be drawn from the table is that different turbulence statistics require different computational lengths to achieve convergence. Results obtained seemed to indicate that statistics in the near-wall region are less sensitive to short domain lengths. To study turbulence statistics in the outer region, the minimum pipe length required appears to scale better in terms of pipe radius rather than using viscous

TABLE III. Summary of estimated minimum computational pipe length required for convergence of different turbulence statistics for $Re_\tau \approx 170$ and 500. The second column displays minimum length in pipe radius (δ) and the last column in viscous wall unit ($^+$). For the one-dimensional energy spectra statistics, the minimum length to obtain converged results for $r^+ < 20$ is stated in the brackets ( ).

	Min length (δ)		Min length ($^+$)	
Turbulence statistics	$Re_\tau = 170$	$Re_\tau = 500$	$Re_\tau = 170$	$Re_\tau = 500$
Mean velocity profile	2π	π	1000	1500
Turbulence intensity	4π	2π	2100	3100
Two-point correlations at $r^+ = 15$	8π	4π	4300	6300
Two-point correlations at $r/\delta = 0.9$	8π	8π	4300	12300
Cross correlations	8π	4π	4300	6300
1*d* energy spectra ($r^+ < 20$)	$8\pi(8\pi)$	$8\pi(4\pi)$	4300(4300)	12300(6300)

length scale. In order to isolate the effects of streamwise periodic boundary conditions on turbulence statics, a proposed pipe length of $8\pi\delta$ appears adequate for all statistics to converge (up to the Reynolds number in this study). The proposed length is by no surprise the same as the domain length advocated by workers such as Hoyas and Jiménez[18] and del Álamo *et al.*[19]

ACKNOWLEDGMENTS

The authors gratefully acknowledge the financial support of the Australian Research Council and the computational resources of the Australian Partnership for Advanced Computing (MAS Grant Nos. p46, m45, and d77) and the Victorian Partnership for Advanced Computing (Project Nos. pMelb0037 and pMelb0061).

[1] P. Moin and K. Mahesh, "Direct numerical simulation: A tool in turbulence research," Annu. Rev. Fluid Mech. **30**, 539 (1998).
[2] S. A. Orszag and G. S. Patterson, "Numerical simulation of three-dimensional homogeneous isotropic turbulence," Phys. Rev. Lett. **28**, 76 (1972).
[3] A. J. Favre, J. J. Gaviglio, and R. J. Dumas, "Space-time double correlations and spectra in a turbulent boundary layer," J. Fluid Mech. **2**, 313 (1957).
[4] A. A. Townsend, *The Structure of Turbulent Shear Flow* (Cambridge University Press, Cambridge, 1956).
[5] K. C. Kim and R. J. Adrian, "Very large-scale motion in the outer layer," Phys. Fluids **11**, 417 (1999).
[6] I. Marusic, B. J. McKeon, P. A. Monkewitz, H. M. Nagib, A. J. Smits, and K. R. Sreenivasan, "Wall-bounded turbulent flows at high Reynolds numbers: Recent advances and key issues," Phys. Fluids **22**, 065103 (2010).
[7] B. J. Balakumar and R. J. Adrian, "Large-and very-large-scale motions in channel and boundary-layer flows," Proc. R. Soc. London, Ser. A **365**, 665 (2007).
[8] N. Hutchins and I. Marusic, "Evidence of very long meandering features in the logarithmic region of turbulent boundary layers," J. Fluid Mech. **579**, 1 (2007).
[9] J. P. Monty, J. A. Stewart, R. C. Williams, and M. S. Chong, "Large-scale features in turbulent pipe and channel flows," J. Fluid Mech. **589**, 147 (2007).
[10] J. P. Monty, N. Hutchins, H. C. H. Ng, I. Marusic, and M. S. Chong, "A comparison of turblent pipe, channel, and boundary layer flows," J. Fluid Mech. **632**, 431 (2009).
[11] J. Kim, P. Moin, and R. Moser, "Turbulence statistics in fully developed channel flow at low Reynolds number," J. Fluid Mech. **177**, 133 (1987).
[12] J. G. M. Eggels, F. Unger, M. H. Weiss, J. Westerweel, R. J. Adrian, R. Friedrich, and F. T. M. Nieuwstadt, "Fully developed turbulent pipe flow: A comparison between direct numerical simulation and experiment," J. Fluid Mech. **268**, 175 (1994).
[13] R. A. Antonia and J. Kim, "Low-Reynolds-number effects on near-wall turbulence," J. Fluid Mech. **276**, 61 (1994).
[14] R. D. Moser, J. Kim, and N. N. Mansour, "Direct numerical simulation of turbulent channel flow up to $Re_\tau = 590$," Phys. Fluids **11**, 943 (1999).
[15] K. Iwamoto, Y. Suzuki, and N. Kasagi, "Reynolds number effect on wall turbulence: Toward effective feedback control," Int. J. Heat Fluid Flow **23**, 678 (2002).
[16] H. Abe, H. Kawamura, and Y. Matsuo, "Direct numerical simulation of a fully developed turbulent channel flow with respect to the Reynolds number dependence," ASME Trans. J. Fluids Eng. **123**, 382 (2001).
[17] H. Abe, H. Kawamura, and H. Choi, "Very large-scale structures and their effects on the wall shear-stress fluctuations in a turbulent channel flow up to $Re_\tau = 640$," ASME Trans. J. Fluids Eng. **126**, 835 (2004).
[18] S. Hoyas and J. Jiménez, "Scaling of the velocity fluctuations in turbulent channels up to $Re_\tau = 2003$," Phys. Fluids **18**, 011702 (2006).
[19] J. C. del Álamo, J. Jiménez, P. Zandonade, and R. D. Moser, "Scaling of the energy spectra of turbulent channels," J. Fluid Mech. **500**, 135 (2004).
[20] C. Wagner, T. J. Hüttl, and R. Friedrich, "Low-Reynolds-number effects derived from direct numerical simulations of turbulent pipe flow," Comput. Fluids **30**, 581 (2001).
[21] X. Wu and P. Moin, "A direct numerical simulation study on the mean velocity characteristics in turbulent pipe flow," J. Fluid Mech. **608**, 81 (2008).
[22] J. F. Morrison, B. J. McKeon, W. Jiang, and A. J. Smits, "Scaling of the streamwise velocity component in turbulent pipe flow," J. Fluid Mech. **508**, 99 (2004).
[23] M. Guala, S. E. Hommema, and R. J. Adrian, "Large-scale and very-large-scale motions in turbulent pipe flow," J. Fluid Mech. **554**, 521 (2006).
[24] J. Jiménez, "Computing high-Reynolds-number turbulence: Will simulations ever replace experiments?" J. Turbul. **4**, 22 (2003).
[25] H. M. Blackburn and S. J. Sherwin, "Formulation of a Galerkin spectral element-Fourier method for three-dimensional incompressible flows in cylindrical geometries," J. Comput. Phys. **197**, 759 (2004).
[26] J. L. Guermond and J. Shen, "Velocity-correction projection methods for incompressible flows," SIAM (Soc. Ind. Appl. Math.) J. Numer. Anal. **41**, 112 (2003).
[27] G. E. Karniadakis, M. Israeli, and S. A. Orszag, "High-order splitting methods for the incompressible Navier–Stokes equations," J. Comput. Phys. **97**, 414 (1991).
[28] R. A. Antonia, M. Teitel, J. Kim, and L. W. B. Browne, "Low-Reynolds-number effects in a fully developed turbulent channel flow," J. Fluid Mech. **236**, 579 (1992).
[29] J. Jiménez and A. Pinelli, "Autonomous cycle of near-wall turbulence," J. Fluid Mech. **389**, 335 (1999).
[30] J. C. del Álamo and J. Jiménez, "Spectra of the very large anisotropic scales in turbulent channels," Phys. Fluids **15**, L41 (2003).
[31] S. Toh and T. Itano, "Interaction between a large-scale structure and near-wall structures in channel flow," J. Fluid Mech. **524**, 249 (2005).
[32] S. Satake, T. Kunugi, and R. Himeno, in *Lecture Notes in Computer Science 1940, High Performance Computing*, edited by M. Valero *et al.* (Springer, Berlin, 2000), pp. 514–523.
[33] M. M. Metzger and J. C. Klewicki, "A comparative study of near-wall turbulence in high and low Reynolds number boundary layers," Phys. Fluids **13**, 692 (2001).

[34]I. Marusic and G. J. Kunkel, "Streamwise turbulence intensity formulation for flat-plate boundary layers," Phys. Fluids **15**, 2461 (2003).
[35]D. B. De Graaff and J. K. Eaton, "Reynolds number scaling of the flat-plate turbulent boundary layer," J. Fluid Mech. **422**, 319 (2000).
[36]B. Ganapathisubramani, N. Hutchins, W. T. Hambleton, E. K. Longmire, and I. Marusic, "Investigation of large-scale coherence in a turbulent boundary layer using two-point correlations," J. Fluid Mech. **524**, 57 (2005).
[37]G. L. Brown and A. S. W. Thomas, "Large structure in a turbulent boundary layer," Phys. Fluids **20**, S243 (1977).
[38]I. Marusic, G. J. Kunkel, and F. Porté-Agel, "Experimental study of wall boundary conditions for large eddy simulation," J. Fluid Mech. **446**, 309 (2001).
[39]I. Marusic and W. D. Heuer, "Reynolds number invariance of the structure inclination angle in wall turbulence," Phys. Rev. Lett. **99**, 114504 (2007).
[40]C. R. Smith and S. P. Metzler, "The characteristics of low-speed streaks in the near-wall region of a turbulent boundary layer," J. Fluid Mech. **129**, 27 (1983).
[41]N. Hutchins and I. Marusic, "Large-scale influences in near-wall turbulence," Philos. Trans. R. Soc. London, Ser. A **365**, 647 (2007).